S1 Extensive model Description

S1.1 Introduction

NUCOM-tundra (NUCOM = NUtrient cycling and COMpetition model) is based on previous NUCOM models for heathlands, forests and peat bogs (Berendse 1988, 1994a and 1994b, Van Oene et al. 1999, Heijmans et al. 2008). The tundra ecosystem model simulates the biomass of three plant functional types (PFTs) and carbon, nitrogen and water dynamics in Arctic tundra ecosystems with a daily time step. The three PFTs included are mosses, graminoids and deciduous dwarf shrubs. Mosses are simulated as a layer that covers the soil surface with a variable thickness. The PFTs compete with each other for light and nutrients. Nitrogen cycling is included to determine nutrient availability for the PFTs. Furthermore, soil moisture status influences PFT growth; therefore a simple hydrological module is included in the model. The soil profile consists of a top soil organic layer and deeper mineral layers. Soil temperatures and active layer thickness (ALT) determine the speed and depth till which biological soil processes occur. These soil processes include decomposition of soil organic material, nitrogen mineralization and denitrification, which affect plant nutrient availability and ecosystem carbon storage.

NUCOM-tundra simulates relatively homogeneous vegetation on the m^2 scale. The parameter values for graminoids and dwarf shrubs were as much as possible derived for *Eriophorum vaginatum* and *Betula nana* respectively, which are both common plant species in Low-Arctic tundra vegetation. For mosses, parameter values were used and calibrated for non-*Sphagnum* mosses. The model requires daily average, minimum and maximum air temperature (T$_{av}$, Tmin, Tmax), and daily precipitation (Prec) as input. Throughout the model, it is assumed that half of the biomass and litter dry weight consists of carbon.

S1.2 Vegetation: Growth and Mortality

S1.2.1 Vegetation overview

NUCOM-tundra essentially simulates the biomass and nitrogen content dynamics of three PFTs: moss, graminoids and dwarf shrubs. Growth, equivalent to net primary production (NPP), of all PFTs is determined by temperature, soil moisture, light and potential nutrient uptake. Mosses can take up nitrogen by nitrogen fixation and nitrogen from atmospheric deposition, as well as from the upper centimetre of the top soil layer. The vascular plants, graminoids and dwarf shrubs, take up nitrogen throughout the active soil profile and can use nitrogen from an internal storage (Fig. S1.1). Part of the nitrogen in dying leaf and root material is reallocated to this nutrient storage.

S1.2.2 Dynamics of plant biomass and N content

Changes in total biomass and total nitrogen content in moss depend on the balance of actual growth and mortality:

$$\frac{d\,(Biom_{moss})}{d\,t} = Gact_{moss} - (mort_{moss} * Biom_{moss}) \tag{S1}$$

$$\frac{d\,(N_{moss})}{d\,t} = Nactuptake_{moss} - (mort_{moss} * N_{moss}) \tag{S2}$$

where $Biom_{moss}$ is the moss biomass (g m^{-2}), $Gact_{moss}$ the actual moss growth (g m^{-2} day^{-1}), $mort_{moss}$ the fraction of moss biomass that dies per day. N_{moss} is the nitrogen content of the moss layer (g m^{-2}) and $Nactuptake_{moss}$ is the actual nitrogen uptake of mosses (g m^{-2} day^{-1}).

The biomass and nitrogen content of graminoids and dwarf shrubs are separated into three different plant parts: fine roots,
10   stems (including coarse roots and rhizomes) and leaves. Consequently, the biomass and nitrogen content are updated per plant part:

$$\frac{d\,(plantpart)}{d\,t} = (Gact * Kallo) - (mort * plantpart) \tag{S3}$$

$$\frac{d\,(Nplantpart)}{d\,t} = (Nactuptake * Kallo) - (mort * Nplantpart) \tag{S4}$$

where $plantpart$ and $Nplantpart$ are the biomass and nitrogen content of the plant part (either roots, stems or leaves) in g m^{-2}, $Gact$ the actual growth (g m^{-2} day^{-1}), $Kallo$ (-) the allocation of growth to the specific plant part and $mort$ (day^{-1}) the mortality (fixed fraction) of the specific plant part.

Additionally, in graminoids and dwarf shrubs, nitrogen is reallocated to and kept in storage. Nitrogen is transferred to the
20   storage from dying plant roots and leaves. The nitrogen in the storage can then be used for plant growth, particularly early in the growing season when most of the soil is still frozen. The amount of nitrogen in the storage depends on the balance of reallocation and uptake of nitrogen from storage:

$$\frac{d\,(Nstorage)}{d\,t} = Krear * (mortr * Nroot) + Kreal * (mortl * Nleaf) - Nactuptake_{sto} \tag{S5}$$

25   in which $Nstorage$ is the amount of stored nitrogen (g m^{-2}), $Krear$ and $Kreal$ the reallocation rates of nitrogen from dying roots and leaves respectively, $mortr$ and $mortl$ the mortality rates of roots and leaves respectively (day^{-1}), $Nroot$ and $Nleaf$ the nitrogen content in roots and leaves respectively (g m^{-2}) and $Nactuptake_{sto}$ the amount of nitrogen that is used from the storage for plant growth (g m^{-2} day^{-1}).

S1.2.3 Actual growth and Nutrient uptake

Actual growth takes place when growing conditions (light, temperature, soil moisture) allow for plant growth, defined as potential growth $Gpot$, and sufficient nitrogen is available. The actual growth and actual nitrogen uptake for all PFTs are calculated according to Eq. S6 and S7, respectively.

$$Gact \begin{cases} Gpot & \text{if } Npotuptake > N_{\min} * Gpot \\ \frac{Npotuptake}{N_{\min}} & \text{if } Npotuptake < N_{\min} * Gpot \end{cases} \tag{S6}$$

$$Nactuptake \begin{cases} Npotuptake & \text{if } Npotuptake < N_{max} * Gpot \\ N_{max} * Gpot & \text{if } Npotuptake > N_{max} * Gpot \end{cases} \tag{S7}$$

where $Gact$ is the actual growth (g m^{-2} day^{-1}), $Gpot$ the potential growth (g m^{-2} day^{-1}), $Nactuptake$ and $Npotuptake$ the actual and potential nitrogen uptake respectively (g m^{-2} day^{-1}), N_{min} and N_{max} the minimum and maximum amount of nitrogen in g that can be taken up per g biomass growth.

The dispersal of spores and seeds is simulated by adding a small biomass to the actual growth for all PFTs during every time step. The biomass of dispersed spores and seeds is defined by the parameter *seedbiom*. This is implemented in NUCOM-tundra to ensure that establishment of PFTs is enabled in simulations where the environmental conditions become suitable for PFT growth.

In vascular plants, the actual growth (*Gact*) and nitrogen uptake (*Nactuptake*) are allocated towards fine roots, stems and leaves. The allocation to roots, stems and leaves is determined by the allocation parameters values of *Kallor*, *Kallow* and *Kallol* respectively. These allocation parameters differ between graminoids and dwarf shrubs and have been calibrated using field biomass data of plant parts (S4).

S1.2.4 Potential nutrient uptake and Root distribution

The potential nutrient uptake is calculated differently for mosses and vascular plants. Mosses can take up nitrogen from atmospheric nitrogen deposition (fixed rate), by nitrogen fixation (fixed rate) and from the available nitrogen pool in the top centimetre of the soil profile. Graminoids and shrubs can use nutrients that were stored by reallocation and they compete with each other for available nutrients in the soil profile according to Eq. S8 and S9.

$$Npotuptake_g = \frac{Nstorage_g}{dt} + \sum_{i=orglay}^{i=maxlayer} \frac{SRL_g * Biomr_{gi}}{SRL_g * Biomr_{gi} + SRL_s * Biomr_{si}} * \frac{N_{ai}}{dt} \tag{S8}$$

$$Npotuptake_s = \frac{Nstorage_s}{dt} + \sum_{i=orglay}^{i=maxlayer} \frac{SRL_s * Biomr_{si}}{SRL_s * Biomr_{si} + SRL_g * Biomr_{gi}} * \frac{N_{ai}}{dt} \tag{S9}$$

where $Npotuptake_g$ and $Npotuptake_s$ are the potential amounts of nitrogen that can be taken up by graminoids and shrubs respectively (g m^{-2} day^{-1}), $Nstorage_g$ and $Nstorage_s$ are the amounts of nitrogen that are stored in graminoids and shrubs respectively (g m^{-2}), *orglay* the organic layer, *maxlayer* is the deepest mineral layer, SRL_g and SRL_s the specific root length of graminoids and shrubs respectively (m g^{-1}), $Biomr_{gi}$ and $Biomr_{si}$ the root biomass of graminoids and shrubs in layer i respectively (g m^{-2}) and N_{ai} the available nitrogen in layer i (g m^{-2}). There is no limit to the amounts of nutrients that can be transferred from the storage or the soil to the plant organs for growth on a single day.

Vascular plants can use nitrogen from their storage and take up nitrogen from the soil profile. If the potential nitrogen uptake is larger than the maximum nitrogen uptake ($N_{max}*Gpot$), nitrogen is first taken up from the soil profile. The nutrient storage is only used when the soil does not provide sufficient nitrogen, for example at the start of the growing season when the soil is still mostly frozen.

The nitrogen uptake per soil layer is calculated by the proportion of roots in that layer. Therefore, the model calculates for both graminoids and dwarfs shrubs its root distribution. The vertical fine root distribution is calculated for the organic and mineral layers based on the position of the layers in the soil profile and using a rooting depth coefficient (Gale and Grigal, 1987; Jackson et al., 1996):

$$Biomr_i = \left((1 - \beta^{endd}) - (1 - \beta^{startd})\right) * Biom_{root} \tag{S10}$$

where $Biomr_i$ is the uncorrected root biomass in layer i (g m^{-2}), β the rooting depth regression coefficient, *endd* and *startd* the start depth and end depth of the soil layer in cm respectively and $Biom_{root}$ the total fine root biomass (g m^{-2}) of the PFT. The model assumes that all fine root biomass is present in the active layer. Consequently, the root biomass per layer is corrected by proportionally redistributing fine root biomass from frozen layers towards the active layers.

S1.2.5 Potential Growth

PFT growth in NUCOM-tundra is restricted by nutrient availability, moisture conditions, temperature and light availability. Potential growth in NUCOM-tundra is defined as the maximum growth when nutrients are not limiting. Consequently, the potential growth of the PFTs is determined by temperature, light availability and moisture conditions according to Eq. S11.

$$Gpot = Gmax * fwc * fT * LI \tag{S11}$$

where $Gpot$ is the potential growth (g m^{-2} day^{-1}) and $Gmax$ the maximum growth under optimal conditions (g m^{-2} day^{-1}). *fwc*, *fT* and *LI* are reduction functions for moisture, temperature and light interception respectively. These functions range between 0 and 1, where a value of 0 limits PFT growth completely and a value of 1 means that the factor is not limiting plant growth.

5 *Moisture conditions*

fwc is calculated based on the volumetric water content in the upper 10cm of the soil following a trapezoidal function also used in the NUCOM-bog model (Heijmans et al., 2008):

$$fwc \begin{cases} 0 & \text{if } w < w_{min} \\ \frac{w - w_{min}}{w_{low} - w_{min}} & \text{if } w_{min} < w < w_{low} \\ 1 & \text{if } w_{low} < w < w_{high} \\ \frac{w - w_{max}}{w_{high} - w_{max}} & \text{if } w_{high} < w < w_{max} \\ 0 & \text{if } w > w_{max} \end{cases} \tag{S12}$$

in which w is the volumetric water content in the upper 10cm of the soil profile in %, w_{min} and w_{max} the lower and upper moisture boundaries in % respectively between which soil moisture enables PFT growth and w_{low} and w_{high} the lower and upper moisture boundaries in % respectively between which soil moisture enables maximum PFT growth.

Temperature

The temperature reduction function *fT* is calculated with a similar formula as for moisture conditions, based on daily average air temperature T_{av}:

$$fT \begin{cases} 0 & \text{if } T_{av} < T_{min} \\ \frac{T_{av} - T_{min}}{T_{low} - T_{min}} & \text{if } T_{min} < T_{av} < T_{low} \\ 1 & \text{if } T_{av} > T_{low} \end{cases} \tag{S13}$$

where T_{min} (^{0}C) is the minimum air temperature which enables growth and T_{low} (^{0}C) is the minimum air temperature enabling maximum PFT growth.

Light availability

Graminoids and dwarf shrubs compete with each other for the incoming light, whereas mosses intercept the remaining light that reaches the soil surface. It is assumed that graminoids and dwarf shrubs are equally tall. The fraction of light that is taken up by graminoids and dwarf shrubs is calculated by Eq. S14 and S15 respectively, using the Lambert-Beer equation and following Van Oene et al. (1999).

$$LI_g = \frac{Kext_g * LAI_g}{Kext_s * LAI_s + Kext_g * LAI_g} * L_a * (1 - e^{-Kext_s * LAI_s - Kext_g * LAI_g}) \tag{S14}$$

$$LI_s = \frac{Kext_s * LAI_s}{Kext_g * LAI_g + Kext_s * LAI_s} * L_a * (1 - e^{-Kext_g * LAI_g - Kext_s * LAI_s}) \tag{S15}$$

where LI_g and LI_s are the light interception fractions of graminoids and shrubs respectively and LAI_g and LAI_s the leaf area indices of graminoids and shrubs respectively (m^2 m^{-2}). $Kext_g$ and $Kext_s$ are the light extinction coefficients of graminoids and shrubs, respectively. L_a is the total available light. As the light interception represents a fraction of total incoming light, L_a is set to 1.

Leaf area index LAI is determined by the specific leaf area and the leaf biomass:

$$LAI = Biom_{leaf} * SLA \tag{S16}$$

where LAI is the leaf area index in m^2 m^{-2}, $Biom_{leaf}$ is the leaf biomass (g m^{-2}) and SLA the specific leaf area (m^2 g^{-1}). The specific leaf area differs for graminoids and shrubs.

The light that is not intercepted by the vascular plants reaches the ground surface and is available for mosses. The light availability for moss LI_m is therefore dependent on the light interception of both graminoids (LI_g) and shrubs (LI_s):

$$LI_m = L_a - (LI_g + LI_s) \tag{S17}$$

S1.2.6 Mortality and reallocation

At every time step, a fixed fraction of moss ($mort_{moss}$) biomass dies and the dead biomass is added to the moss litter pool (Eq. S1 and S20) in the soil organic layer. For the vascular plant PFTs, mortality rates have been defined for roots ($mort_r$), stems ($mort_s$) and leaves ($mort_l$) separately. Part of the nitrogen is reallocated from dying vascular plant roots and leaves towards the nitrogen storage. This reallocation fraction is defined by $Krear$ and $Kreal$ for dying roots and leaves respectively. Both the mortality and reallocation parameter values differ between graminoids and dwarf shrubs.

As stems have a much lower mortality rate in comparison to fine roots and leaves, stems may persist for a very long time even when growing conditions have become unsuitable for plant growth, e.g. for dwarf shrubs after thaw pond development. Therefore, to prevent persistent woody plant parts in graminoids and shrubs, the mortality of stems is increased to a higher mortality rate (defined by $maxmort_s$) when the actual growth has been smaller than 1 g in the previous two years.

In mosses, mortality can also occur if the moss layer grows too high. The moss layer should have a height of between 0.005 m and 0.045 m. If the moss layer exceeds this height, it is assumed that the surplus dies due to lack of light and this

additional litter is added to the moss litter pool in the organic soil layer. The height of the moss layer (m) is calculated by multiplying the moss biomass (g m^{-2}) by moss bulk density (BD_m, g m^{-3}).

S1.3 Soil

S1.3.1 Soil overview

5   The soil is divided into an organic layer and 10 mineral soil layers. The height of the organic layer is dynamic and depends on the amount of litter. The deeper soil consists of 10 mineral layers (the number of layers is defined by parameter *maxlayer*) with a fixed height of 0.10 m (parameter *layerdepth*), which also contain (small) litter pools

The litter pools are defined for both carbon (*Clitter*) and nitrogen (*Nlitter*) and for mosses and plant parts in both graminoids and dwarfs shrubs. Litter pools of moss, vascular plant stems and vascular plant leaves make up the organic layer in the top

10   part of the soil profile. Root litter pools are defined for every soil layer separately for both graminoids and dwarf shrubs. Several soil processes are simulated in NUCOM-tundra, relating to both nitrogen and carbon cycling (Fig. S1.2). The carbon in litter pools can be decomposed and released as CO_2. Nitrogen can be mineralized, after which it is added to the available nitrogen pool for plants (*Na*). Under wet conditions, however, the available nitrogen can also be denitrified and released as N_2 to the atmosphere. All these microbial soil processes depend on soil temperature. Furthermore, nitrogen can leach through

15   the soil profile towards deeper layers. The calculations for these processes are presented in this part of the model description. In the equations general terms are used which are valid for mosses and all vascular plant parts. Note however, that soil processes are separately simulated for each litter pool with different parameter values for e.g. relative decomposition rate (day^{-1}). NUCOM-tundra does not take litter age into account, so no age classes are used to calculate the speed of soil processes.

20   **S1.3.2 Dynamics of soil organic carbon and nitrogen pools and available nitrogen**

The total available nitrogen is updated for every soil layer according to Eq. S19:

$$\frac{d\,(N_a)}{d\,T} = mineralization + Nleach_{lay[i-1]} - denitrification - Nuptake_{soil} - Nleach_{lay[i]} \qquad \text{(S19)}$$

25   where *Na* is the amount of available nitrogen (g m^{-2}) in a specified soil layer and *Nuptake$_{soil}$* the amount of nitrogen that is taken up by the PFTs from that soil layer (g m^{-2} day^{-1}). *Mineralization* and *denitrification* are calculated according to Equations S25 and S26 respectively. *Nleach$_{lay[i-1]}$* is the amount of available nitrogen leaching from the above soil layer (g m^{-2} day^{-1}), whereas *Nleach$_{lay[i]}$* is the amount of nitrogen leaching into the underlying soil layer (Eq. S29).

The litter carbon and nitrogen pools change according to Eq. S20 and S21, respectively:

$$\frac{d\ (Clitter)}{d\ T} = (\frac{1}{2} * mort * plantpart) - decomposition \tag{S20}$$

$$\frac{d\ (Nlitter)}{d\ T} = (1 - Krea)(mort * Nplantpart) - mineralization \tag{S21}$$

where *mort* is the relative mortality rate (day^{-1}), *plantpart* the biomass of a specified plant part (g m^{-2}) and *Nplantpart* the nitrogen content of a specified plant part (g m^{-2}). *Krea* is the reallocation fraction. Nitrogen is partly reallocated from dying

5   vascular plant leaves and roots towards a nutrient storage. Decomposition and mineralization are calculated according to Eq. S23 and S25 respectively.

The height of the dynamic organic layer is then determined by the amount of litter present in this layer according to Eq. S22:

10    $$Orglay_{depth} = ((Clitterm + Clitterg_{(s+l+r[org])} + Clitters_{(s+l+r[org])}) * 2)/BD_{org} \tag{S22}$$

where $Orglay_{depth}$ is the height of the organic layer in m, *Clitterm* the moss litter, $Clitterg_{(s+l+r[org])}$ and $Clitters_{(s+l+r[org])}$ the stem litter, leaf litter and litter from roots present in the organic layer for graminoids and shrubs respectively in g C m^{-2}. BD_{org} is the organic matter bulk density (g m^{-3}). In the equation, the carbon litter biomass is multiplied by two as carbon is

15   assumed to make up half of the total litter biomass.

S1.3.3 Soil processes

Decomposition
Decomposition is determined by the amount of carbon present in the litter pool, the relative decomposition rate of the litter type and soil temperature:

$$decomposition = Clitter * kdec * fTs \tag{S23}$$

where *decomposition* is the amount of carbon that is decomposed (g m^{-2} day^{-1}), *Clitter* the pool of litter carbon (g m^{-2}), *kdec* the relative decomposition rate under optimal conditions (day^{-1}) and *fTs* the temperature reduction factor calculated with Eq.

25   S24. Note that decomposition is calculated for every litter pool in every layer separately. So, litter pools and decomposition rates are defined for moss, graminoid roots, stems and leaves, and shrub roots, stems and leaves.

As soil temperature has a large influence on decomposition, the decomposition rates are adjusted by factor *fTs*. This temperature factor is calculated for every soil layer based on the soil temperature according to Eq. S24 (Kirschbaum, 1995):

$$fTs = e^{-3.764+0.204*soilT*\left(1-0.5\left(\frac{soilT}{36.9}\right)\right)} \tag{S24}$$

where *fTs* is the rate constant of soil processes and *soilT* the soil temperature in a specific layer (^{0}C).

Mineralization

Mineralization of nitrogen in litter pools depends on the N:C ratio of the litter and the decomposition rate according to Eq. S25.

$$mineralization = \left(\frac{Nlitter}{Clitter} - NCcrit\right) * \left(\frac{1}{1-e^{asseff}}\right) * Clitter * kdec * fTs \tag{S25}$$

where *mineralization* is the nitrogen mineralization rate (g m^{-2} day^{-1}), *Nlitter* the nitrogen pool (g m^{-2}), C litter the carbon pool (g m^{-2}), *NCcrit* the critical N:C ratio for N mineralisation (g g^{-1}), *asseff* the microbial assimilation efficiency, *kdec* the relative decomposition rate (day^{-1}) and *fTs* the temperature reduction factor calculated according to Eq. S24. The relative decomposition rate *kdec* is defined for every plant part separately.

Denitrification

Denitrification of plant available nitrogen depends on the available nitrogen concentration, soil moisture, temperature and pH as described by Heinen (2006). The actual denitrification is calculated according to Eq. S26.

$$denitrification = \alpha * N_a * f_S * f_{Td} \tag{S26}$$

where *denitrification* is the denitrified amount of nitrogen per day (g m^{-2} day^{-1}), α the denitrification rate under optimal conditions (day^{-1}), Na the available nitrogen pool (g m^{-2}), f_S and f_{Td} reduction functions for water and temperature respectively.

The reduction function for moisture, f_S is calculated according to Eq. 27:

$$f_S \begin{cases} 0 & \text{if } S < S_{tres} \\ \left(\frac{S-S_{tres}}{S_{\max}-S_{tres}}\right) & \text{if } S_{tres} \leq S \leq S_{max} \\ 1 & \text{if } S_{max} < S \end{cases} \tag{S27}$$

where *S* is the actual fraction of pores in the soil that are water filled. S_{tres} is the threshold fraction of water filled pores that is required for denitrification. S_{max} is the fraction of water filled pores that enables maximum denitrification. As denitrification

occurs under anaerobic conditions, S_{max} equals 1. The fraction of water filled pores (S) is calculated by dividing the water content of a layer by the maximum capacity of that layer.

The reduction function for soil temperature is calculated according to Eq. S28 (Heinen, 2006):

$$f_{Td} = Q_{10}^{\left(\frac{soilT - T_{ref}}{10}\right)} \tag{S28}$$

in which *soilT* is the soil temperature (^{0}C), Q_{10} the increase factor for a soil temperature rise of 10 ^{0}C and T_{ref} the reference temperature value at which denitrification rates are not limited by temperature (^{0}C).

Nutrient leaching

Leaching of available nutrients into the mineral layers is calculated by two components (Eq. S29). Firstly, the percolation of water is assumed to cause nutrient leaching to deeper layers, and, secondly, nutrient leaching occurs with a small fixed rate.

$$Nleach_{lay[i]} = \frac{actPer_{lay[i]}}{wc_{lay[i-1]}} * Na_{lay[i]} + leachr * Na_{lay[i-1]} \tag{S29}$$

where $Nleach_{lay[i]}$ is the actual amount of plant available nitrogen that leaches into layer i (g m^{-2} day^{-1}), $actPer_{lay[i]}$ the actual percolation into layer i (mm day^{-1}), $wc_{lay[i-1]}$ the water content in layer i-1 (mm), $Na_{lay[i]}$ and $Na_{lay[i-1]}$ the available nitrogen in layers i and i-1 respectively (g m^{-2}) and *leachr* (day^{-1}) a fixed nutrient leaching rate. Note that, when calculating nutrient leaching into layer 1, layer 0 refers to the organic layer. Total nutrient leaching can never exceed a fixed maximum rate, which is defined as $leachr_{max}$ (day^{-1}).

S1.3.4 Soil Temperature and Active Layer Thickness

Seasonal variations in soil temperatures and active layer thickness are highly dependent on air temperature (e.g. Kane et al., 1991). For simulating soil temperatures we used a simple linear regression approach, with air temperature as input. Soil temperature at 10cm depth is calculated by a method designed by Zheng et al. (1993). The soil temperatures for deeper layers (with steps of 10cm) were calculated by similar simple linear regression based on the temperature of the above layer. Active layer depth is calculated by interpolation between the deepest thawed layer and the highest frozen layer. The regression soil temperature model was calibrated using soil temperature data from the Chokurdakh Tundra Station for depths ranging from 2 till 80cm for 2013 and 2014. Soil temperature data from 2013 was used to calibrate parameters, whereas the data for 2014 was used to check whether the simulated soil temperatures were in agreement with the observed soil temperatures. Calibration was only done for soil temperatures above 0^{0}C, as differences in freezing soil temperature values

have only a negligible influence on model outputs. No attempt was done to simulate the zero curtain phase at the start of the winter season.

After calibration, the soil temperature at a depth of 10cm was calculated using Eq. S30 (adjusted from Zheng et al., 1993).

$$SoilT_{10cm} = (Tair_{eleven[t]} - Tair_{eleven[t-1]}) * M + Tair_{eleven[t]} * a_{10} + b_{snow} \tag{S30}$$

where $SoilT_{10cm}$ is the soil temperature at 10cm depth (^{0}C), $Tair_{eleven[t]}$ and $Tair_{eleven[t-1]}$ the eleven day average air temperature of this and previous day respectively (^{0}C), M a rate scale which was set to 0.5, a_{10} a linear regression coefficient set to 0.4 and b_{snow} a correction factor for snow presence used to calculate the delayed increase of soil temperatures after snow presence (^{0}C). b_{snow} is calculated according to Eq. S31:

$$\frac{d\,(b_{snow})}{dt} = \begin{cases} b_{change} & if\ Snow > 0 \\ -b_{change} & if\ Snow = 0 \end{cases} \tag{S31}$$

where b_{snow} is the correction factor on soil temperature at 10cm depth (°C), b_{change} the change of the correction factor per time step (°C) and $Snow$ the amount of water that is present in a the snow pack (mm). b_{snow} can only range between -20°C and 0°C. The correction factor accounts for the delay of temperature rise after snowmelt.

The soil temperatures for deeper layers were calculated according to Eq. S32:

$$SoilT_i = SoilT_{eleven(i-1)} * a_i + b_i \tag{S32}$$

Where $SoilT_i$ is the soil temperature at depth i (°C), $SoilT_{eleven(i-1)}$ the average soil temperature over the previous eleven days of the above layer (°C), a_i a regression coefficient specific for depth i and b_i a correction factor specific for depth i (°C) (values of a_i and b_i in Table S1.1). Depth i represent depths ranging from 20 till 140cm, using in between steps of 10cm. To be able to calculate the temperature in the upper 10cm, a soil surface temperature was derived from $SoilT_{10cm}$.

The comparison of simulated and observed soil temperatures at 10, 20, 40 and 80cm depth for 2013 and 2014 is presented in Fig. S1.3. Daily precipitation (to calculate snow) and air temperature data from the meteo station at Chokurdakh were used as model input. The field data of 2013 was used to calibrate the model and, consequently, simulated soil temperatures during the growing season can be compared to observed values. For 2014, simulated soil temperatures are too low for 20 and 40 cm depths. The timing at which those layers thaw is, however, highly comparable to measured values. Although the simple soil

temperature model is thus not able to perfectly simulate soil temperatures, it captures, due to its air temperature dependence, seasonal and year to year variations in active layer thickness.

S1.4 Hydrology

S1.4.1 Hydrology Overview

5   The hydrological part of the model simulates snow depth, surface water height and the volumetric water content in the organic and mineral soil layers using a daily time step (Fig. S1.4). Precipitation falls as rain or snow. Both rain and snowmelt influence surface water height. Infiltration of water occurs from the surface water into the organic layer, unless it is frozen. From there, water percolates to deeper mineral layers. Infiltration and percolation of water is calculated using field and maximum moisture capacities, which are defined for organic and mineral soils separately.

10   Horizontal outflow of water occurs by surface water runoff. Inflow of surface water and lateral drainage of water in and out of the organic layer is simulated as well. Besides surface runoff, water is also lost from the system by evapotranspiration.

The average volumetric water content of the upper 10cm (w) of the soil profile is calculated as the moisture factor that influences plant growth.

S1.4.2 Dynamics of snow, surface water and soil moisture

15   The height of the surface water is determined by several hydrological processes. Surface water height increases by snowmelt, rainfall and surface water inflow, whereas the surface water height decreases due to evapotranspiration, infiltration and surface water outflow:

$$\frac{d\,(Surfacewater)}{dt} = Snowmelt + Rain + runoff_{in} - ET_s - actInf_{org} - runoff_{out} \tag{S33}$$

where $Surfacewater$ is the amount of water on the soil surface (mm), $Snowmelt$ the amount of melted snow (mm day-1), rain
20   the amount of rainfall (mm day^{-1}), ET_s the evapotranspiration from the surface water (mm day^{-1}), $actInf_{org}$ the amount of water that infiltrates into the organic layer (mm day^{-1}) and $runoff_{in}$ and $runoff_{out}$ the surface water inflow and outflow respectively (mm day^{-1}).

The water content of the organic layer depends on water infiltration, percolation, lateral drainage (named interflow) and evapotranspiration:

25   $$\frac{d\,(wc_{org})}{dt} = actInf_{org} + interflow_{in} - ET_{org} - actPer_{lay[1]} - interflow_{out} \tag{S34}$$

where wc_{org} is the water content of the organic layer (mm), $actInf_{org}$ the amount of water that infiltrates into the organic layer (mm day^{-1}), ET_{org} the evapotranspiration from the organic layer (mm day^{-1}), $actPer_{lay[1]}$ the percolation of water from the organic layer into the top mineral layer (mm day^{-1}) and $interflow_{in}$ and $interflow_{out}$ the horizontal water flows in and out the organic layer respectively (mm day^{-1}).

5   Percolation and evapotranspiration determine water changes in the mineral layers:

$$\frac{d\,(wc_{lay[i]})}{dt} = actPer_{lay[i]} - ET_{min[i]} - actPer_{lay[i+1]} \tag{S35}$$

where $wc_{lay[i]}$ is the water content in mineral layer i (mm), $ET_{min[i]}$ the evapotranspiration from mineral layer i (mm day^{-1}) and $actPer_{lay[i]}$ and $actPer_{lay[i+1]}$ the percolation in and out mineral layer i respectively (mm day^{-1}).

S1.4.3 Snow depth

10   Snow is simulated as a Snow Water Equivalent, which is the actual amount of water that is held by the snow. Snow accumulates when the air temperature is below or equal to 0 ^{0}C, whereas snowmelt occurs with higher temperatures (Eq. S36).

$$Snowmelt = DDF * T_{av} \tag{S36}$$

15   .

where $Snowmelt$ is the amount of water that is released by melting of snow (mm day^{-1}), DDF is a Degree Day Factor used to calculate snowmelt (mm ^{0}C^{-1} day^{-1}) and T_{av} is the average daily air temperature in ^{0}C. The snow water equivalent is updated according to Eq. S37.

$$\frac{d\,(Snow)}{dt} = \begin{cases} Prec & for\ T_{av} \leq 0 \\ Snowmelt & for\ T_{av} > 0 \end{cases} \tag{S37}$$

where $Snow$ is the amount of water in mm that is stored in the snow layer and $Prec$ is the precipitation in mm day^{-1}.

S1.4.4 Evapotranspiration

Potential Evapotranspiration

25   The potential total evapotranspiration is calculated according to the Hargreaves equation (Hargreaves and Allen, 2003):

$$PET = \frac{0.0023}{\lambda} * (T_{av} + 17.8) * \sqrt{Temp_{max} - Temp_{min}} * R_a \tag{S38}$$

where *PET* is the potential evapotranspiration in mm day^{-1}, *Ra* is the extra-terrestrial radiation (MJ m^{-2} day^{-1}), *Temp$_{min}$*, *T$_{av}$* and *Temp$_{max}$* the minimum, average and maximum daily temperature in ^{0}C respectively. λ (Lambda) is the latent heat of vaporization of water in MJ kg^{-1}, and calculated by the average temperature according to Eq. S39.

$$\lambda = 2.501 - 0.002361 * T_{av} \tag{S39}$$

Actual Evapotranspiration

The potential evapotranspiration calculated using Eq. S38 was compared to actual evapotranspiration measured as latent heat flux at the Chokurdakh Tundra Station to examine the relation between actual and potential evapotranspiration. The potential evapotranspiration for Chokurdakh was calculated with solar radiation at 70˚N. Daily mean, minimum and maximum temperatures were obtained for the Chokurdakh weather station (located 70˚ 62' N, 147˚ 88' E; altitude 44.0m) (Klein Tank et al., 2002) located at 27 km from the Kytalyk field station.

The Hargreaves potential evapotranspiration was compared to actual latent heat flux measured at the Kytalyk research site for 772 days in the time period 2003-2011, the dates ranging from April 14 till September 28. Daily potential evapotranspiration was compared to actual heat flux if the measurements covered more than half of that day. The ratio actual:potential evapotranspiration was determined over time (Fig. S1.5).

The potential evaporation calculated with the Hargreaves equation was usually larger than the evapotranspiration measured at the Chokurdakh Tundra Station. To obtain actual evapotranspiration values in NUCOM-tundra, daily potential evapotranspiration calculated with Eq. S38 was multiplied with a correction factor based on the relationship between actual and Hargreaves potential evapotranspiration (Fig. S1.5). Early in the growing season, the actual evapotranspiration is only a small fraction of the calculated Hargreaves potential evapotranspiration, probably because the soil is still mostly frozen. During the growing season, the actual evapotranspiration fraction increases relative to the potential evapotranspiration. At the end of the growing season, in September, the actual evapotranspiration equals and sometimes even exceeds the potential evapotranspiration. The linear regression function for this relationship (Eq. S40) was incorporated in NUCOM-tundra as a correction factor for calculating actual evapotranspiration from Hargreaves potential evapotranspiration:

$$ActET = PET * (0.0056 * dayy - 0.5412) \quad for\ 96\ (Apr\ 6) < dayy < 323\ (Nov\ 11) \tag{S40}$$

in which *ActET* is an estimate of the actual evapotranspiration (mm day^{-1}), *PET* is the Hargreaves potential evapotranspiration (mm day^{-1}) as calculated according to Eq. S38, and *dayy* is the day number in the year, counting from January 1st as day number 1.

Partitioning of evapotranspiration

A predefined fraction determines the proportion of actual evapotranspiration that is contributed to surface evaporation. This evaporation fraction is set to 0.5, so that the total actual evapotranspiration is equally divided into evaporation and transpiration. Evaporation of water occurs from surface water and water in the upper part of the soil profile, which height is set by parameter *evapodepth*. If the available water in these layers is insufficient for evaporation, the deficient amount of water will not evaporate. Transpiration occurs throughout all active soil layers, and in proportion to the fine root biomass present in the different layers. If there is insufficient water in the upper layers for transpiration, more water will be taken from the deeper active layers until the total transpiration value is reached.

S1.4.5 Infiltration and Percolation

Infiltration and percolation to deeper layers occurs when there is an excess of water in upper layers (which is the surface water and the water in excess of field capacity) and when the active deeper layers are not completely water saturated. There is no limit to the amount of water that can infiltrate and percolate during a single day.

The infiltration is defined as the amount of water that infiltrates from the ground surface into the organic layer. First, the maximum amount of water that can infiltrate is calculated using Eq. S41:

$$potInf = (mc_{org} - wc_{org}) + (mc_{\min[1:endl]} - wc_{\min[1:endl]}) \tag{S41}$$

where *potInf* is the maximum amount of water that can infiltrate to reach water saturation in the active soil profile (mm), mc_{org} and mc_{min} the maximum capacity in active organic and mineral layers respectively (mm), wc_{org} and wc_{min} the actual water content in active organic and mineral layers respectively (mm), and *endl* the deepest active layer.

Then, the actual amount of water that infiltrates into the organic layer is calculated:

$$actInf_{org} \begin{cases} potInf & if \ Surfacewater \geq potInf \\ Surfacewater & if \ Surfacewater < potInf \end{cases} \tag{S42}$$

in which *actInf_org* is the actual amount of water that infiltrates into the organic layer in mm day^{-1}, *Surfacewater* is the height of the water above the soil surface in mm, *potInf* is the calculated maximum water infiltration (Eq. S41). Normally the surface water can infiltrate in the organic layer, but it is maximized by the space for water over the thawed soil profile. As a result, surface water is mostly present at the time of snowmelt and shallow active layer thickness.

Percolation is defined as the water that percolates in the mineral layers, either from the organic layer or from an upper mineral layer. The percolation is calculated for all mineral soil layers according to Eq. S43.

$$actPer_{\text{lay}[i]} \begin{cases} = 0 \\ \text{if } \left(wc_{lay[i-1]} + actPer_{lay[i-1]}\right) < fc_{lay[i-1]} \\[8pt] = wc_{lay[i-1]} + actPer_{lay[i-1]} - fc_{lay[i-1]} \\ \text{if } \left(wc_{lay[i-1]} + actPer_{lay[i-1]} - fc_{lay[i-1]}\right) \leq (mc_{lay[i:endl]} - wc_{lay[i:endl]}) \\[8pt] = mc_{lay[i:endl]} - wc_{lay[i:endl]} \\ \text{if } \left(wc_{lay[i-1]} + actPer_{lay[i-1]} - fc_{lay[i-1]}\right) > (mc_{lay[i:endl]} - wc_{lay[i:endl]}) \end{cases} \tag{S43}$$

where *actPerlay* is the actual amount of water that percolates into layer i (mm day-1), *wclay* is the water content in mm, *fclay* is the water content at field capacity (mm) and *mcmin* is the maximum water capacity for mineral soil (mm). Note that when calculating the actual percolation for mineral layer 1, i=0 in the equations refers to the organic layer. Therefore, *actPerlay[0]* equals *actInf$_{org}$* as calculated in Eq. S42.

S1.4.6 Surface water runoff and Interflow

If a water layer on the ground surface is still present after infiltration, surface water runoff occurs with a fixed runoff rate (Eq. S44):

$$runoff_{out} = Surfacewater[t-1] * runoffr \tag{S44}$$

where *runoff$_{out}$* is the amount of water surface runoff (mm day^{-1}), *Surfacewater* the amount of water present on the ground surface (mm) and *runoffr* a fixed water runoff rate (day^{-1}). Lateral water flow out of the organic layer is calculated similarly with a fixed interflow rate:

$$interflow_{out} = (wc_{org}[t-1] - (mc_{org} - fc_{org})) * interflowr \tag{S45}$$

where *interflow$_{out}$* is the amount of water that flows out of the system through the organic layer (mm day^{-1}), *wc$_{org}$*, *mc$_{org}$* and *fc$_{org}$* the actual, maximum and field water capacity of the organic layer (mm) and *interflowr* a fixed interflow rate (day^{-1}).

Runoff$_{in}$ and *interflow$_{in}$* are equal to the *runoff$_{out}$* and *interflow$_{out}$* of the adjacent upslope vegetation type. Interflow and runoff in and out the simulated patch can be switched on and off depending on the position in the landscape in association with the type of vegetation that is simulated. In relatively well-drained landscape positions dominated by shrub vegetation, only water outflow is simulated, whereas in the lowest landscape positions dominated by wet sedge vegetation only water inflow is simulated. In moist in between landscape positions, both water inflow and outflow is simulated.

S1.4.7 Thaw pond formation

A simple module for simulating small-scale collapse or abrupt thaw of ice-rich permafrost, here named thaw pond formation, is incorporated in NUCOM-tundra. Thaw pond formation in NUCOM-tundra occurs at a predefined time step. The occurrence of a collapse means that $runoff_{in}$ and $interflow_{in}$ are, if not yet simulated, activated and doubled and that $runoff_{out}$ and $interflow_{out}$ are inactivated if the surface water does not reach a height of 100mm. The model thus assumes a ground collapse 10cm. Subsequently, $Runoff_{out}$ occurs when the surface water reaches a height of more than 100mm. $runoff_{in}$ and $interflow_{in}$ equal $runoff_{out}$ and $interflow_{out}$ of a simulation of an adjacent upslope landscape position. Thus, when using the thaw pond formation module, only the runoff and interflow values are changed.

S2 Site Description

S2.1 General site description

For this study, many of the data that were used for calibrating, validating and running the NUCOM-tundra model have been collected at the Chokurdakh Scientific Tundra Station (located 70° 49′ N, 147° 29′ E, altitude 10 m), also known as Kytalyk field station. The research station is situated in Wildlife Reserve Kytalyk, located in the lowlands of the Indigirka river, in the north-eastern part of the Sakha Republic (Yakutia), Russian Federation, about 150 km south of the East Siberian Sea (van der Molen, 2007).

The research site is situated in the Low Arctic climate zone and is characterized by thick continuous permafrost with a shallow active layer. The top 10-15cm of the soil is highly organic, whereas the deeper mineral layers consist out of silty clay (Blok et al., 2011). From early June the upper part of the soil thaws, enabling plant growth. During winter, a snow layer accumulates reaching a variable height, ranging between 20 and 70 cm. This snow layer melts in late May – early June, by which the soil becomes mostly water saturated. During the summer, the soil gradually becomes drier as evapotranspiration generally exceeds precipitation (Fig. S2.1).

The vegetation near Chokurdakh is classified as tussock-sedge, dwarf-shrub, moss tundra (G4) and low-shrub tundra (S2) on the circumpolar arctic vegetation map (Walker et al., 2005). The lowland tundra landscape mostly consists of floodplains, drained thaw lake basins and higher plateaus which are Pleistocene remnant surfaces. The field data used in this study have been collected in a former thaw lake which shows a micro topography of slightly elevated shrub patches dominated by *Betula nana* L. (dwarf birch) within a diffuse drainage network of wet depressions dominated by the graminoid species *Eriophorum angustifolium* Honck (Nauta et al. 2015). *Eriophorum vaginatum* L. is co-dominant with *B. nana* in moist tussock tundra vegetation and is also present in wet sites including shallow thaw ponds. The soil surface is overgrown with a layer of mosses and lichens with a height of 4-5cm (Blok et al., 2011).

Temperature and Precipitation data from Chokurdakh Weather Station (WMO station 21946, located 70˚ 62' N, 147˚ 88' E; altitude 44.0m), at 27 km of the field site, for the time period 1981-2010 are presented in Table S2.1 (Klein Tank et al., 2002). Average annual temperature is -13.3 ˚C. Monthly average temperatures range from -33.9 ˚C in January to 10.6 ˚C in July. Annual average precipitation is 203.5 mm, about half of which falls during the growing season (104.6 mm in June-September).

S2.2 Climate change

Climatic change has been observed at Chokurdakh during the last decades. The average annual temperature for the Chokurdakh weather station (WMO station 21946, located 70˚ 62' N, 147˚ 88' E; altitude 44.0m) for 1946-2010 is presented in Fig. S2.2.

Temperature has increased on average 0.0243 ˚C year^{-1} between 1946 and 2010. However, temperature has not increased between 1946 and 1980 (-0.0111 ˚C year^{-1}). For 1981-2010, temperature has increased by 0.0565 ˚C year^{-1}. Climatic warming has been most pronounced in the last decades, as temperature has increased on average 0.2011 ˚C year^{-1} between 1996 and 2010.

5   Annual precipitation is highly variable, ranging from 88mm to 357mm between 1946 and 2010. Trends and correlations between temperature and precipitation are therefore hard to detect and interpret. Precipitation (Fig. S2.3) has on average slightly increased between 1946 and 2010 (0.267 mm year^{-1}). However, a decrease in precipitation has been observed at the Chokurdakh weather station between 1981 and 2010 (average change of -1.127 mm year^{-1}) which was even stronger between 1996 and 2010 (average change of -2.791 mm year^{-1}). There is no correlation ($R^2 = 0.0058$) between mean annual

10   temperature and annual precipitation at the Chokurdakh weather station.

S2.3 NUCOM-tundra weather input

For the model simulations in NUCOM-tundra, weather data between 1954 and 1994 was used as a baseline for the climate scenarios. This period excludes the relatively dry years between 1946 and 1953. Although temperature has slightly increased between 1954 and 1994, the period excludes the most pronounced climate warming that has been observed in recent years.

S3 Initial Values for simulations

All simulations, independently of vegetation type, start with the same initial values for litter pools and soil moisture content in organic and mineral soil layers. Each of the seven carbon litter pools in the organic layer have an initial value of 1500 g which results in an initial thickness of the organic layer of 14 cm. All nitrogen litter pools in the organic layer have an initial

5   value of 50 g, but at the start of the simulation no available nitrogen is yet present in this layer. Initial water content in the organic layer is 80 mm water. Table S3.1 presents the initial values for the moisture and old and root litter pools in the mineral layers. The amount of carbon and nitrogen in the old litter pools varies over the mineral soil layers, with a C:N ratio of about 21 for the upper mineral soil layers similarly as reported in field studies (Marion and Miller, 1982; Sistla et al., 2013). The five vegetation types differ in water flow settings and initial values for biomass of the PFTs (Table S3.2). The

10   initial biomass values of graminoids, dwarf shrubs and mosses are within the range of total dry biomass weights observed at the Chokurdakh Scientific Tundra Station.

S4 Comparison with Field Data

S4.1 Snowdepth

Simulated Snow Water Equivalents were compared with snow height measurements at the Chokurdakh weather station (located 70˚ 62' N, 147˚ 88' E; altitude 44.0 m). Snow depth data at the Chokurdakh weather station were available from July 1944 till the end of 2008 (Klein Tank et al., 2002). These data were compared with model simulations over the same time period, using temperature and precipitation input from the same weather station. The simulated snow water equivalents simulated with NUCOM-tundra were converted into snow heights. The precise conversion of snow water equivalents to snow heights is complicated as snowdepth-precipitation ratios may range from 3:1 till 100:1 (Roebber et al., 2003). This analysis, however, focused on the timing and accumulation of the snow layer, rather than the precise height of the snow layer. Therefore, a constant snowdepth-precipitation ratio of 5:1 was used to convert simulated Snow Water Equivalents into snowpack heights. A correlation coefficient was determined for the period 1 July 1944 till 30 June 2008, including days for which no snow was present in both the simulation and field data.

The accumulation of snow during winter and the duration and timing of snowmelt in spring were very similar among simulated and measured data during the time period 1944-2008 (R^2 = 0.725, n = 16255 days). The simulated and observed snow depths for the time period 2002-2008 are shown in Fig. S4.1. Although there were differences between simulated and measured snow depth, the start of snow accumulation and the time and duration of snow melt were captured very well by the simple snow model. Deviations in year to year maximum snow height between simulated and observed values may be caused by wind driven snow transfers (Essery and Pomeroy, 2004) or by annual differences in snow densities, which can be due to a number of factors including humidity (Roebber et al., 2003).

S4.2 Total biomass, biomass partitioning and fine root distribution in vascular plants

Some growth, allocation and mortality parameter values were calibrated based on field PFT biomass data from the Chokurdakh Tundra Station. Simulated biomass, vertical root distribution and biomass partitioning in different plant parts (roots, stems and leaves) in vascular plants was compared with field data from the Chokurdakh Tundra Station to evaluate model performance.

S4.2.1 Field data collection

Aboveground and belowground biomass was collected and measured for dwarf shrubs and graminoids in both early and late growing season in 2013. Biomass was sampled in eight blocks, each block consisting of three plots representing: vegetation with mainly dwarf shrubs, vegetation with mainly graminoids, and a mixed vegetation. In each plot samples were taken at two positions within the plot. Dry aboveground biomass was weighed for graminoids and shrubs. For shrubs, distinction was made between stems and leaves. Belowground biomass was measured in two or three layers, depending on the depth of the

active layer. The biomass in the soil layers was separated into rhizomes/coarse roots (in NUCOM-tundra considered as part of stems) and fine roots.

S4.2.2 Total biomass and biomass partitioning

Total plant biomass and the partitioning of biomass over the three plant parts from the field collection data was visually compared with data simulated with NUCOM-tundra. For graminoids, only field samples in mixed and graminoid dominated plots were included, whereas for shrubs only samples from mixed and shrub dominated plots were included. Model simulations were performed for all vegetation types under no climate change as described in the main text. Chokurdakh weather data (August 1 1954 till July 31 1994) was used as baseline climate input, which was repeated for the years 1995-2034. Here, the allocation towards the different plant parts was plotted against the total PFT biomass for 31 July in simulated years 1995-2034. For graminoids, simulated moist mixed and wet graminoid dominated vegetation types (vegetation types 2-5), whereas for shrubs moist mixed and dry shrub dominated vegetation types (vegetation types 1-4) were compared to the field data.

Figure S4.2 presents observed and simulated total PFT biomass and partitioning over leaves, stems and fine roots in graminoids and shrubs. Total biomass in the field was in general higher for shrubs (average shrub biomass in shrub dominated plots 1615 g m^{-2} and maximum biomass around 2500 g m^{-2}) than for graminoids (average graminoid biomass in graminoid dominated plots 931 g m^{-2} and maximum biomass around 2000g m^{-2}). The simulated total biomass for both graminoids and shrubs were well in the range of observed biomass (Fig. S4.2). The largest part of graminoid and shrub biomass is in their woody plant parts, which include both stems (in shrubs only) and rhizomes (in both graminoids and shrubs). A smaller proportion of biomass is in roots and leaf biomass is only a small fraction of the total biomass. Model simulations with NUCOM-tundra show a similar division between biomass in roots, stems and leaves in both graminoids and shrubs.

The field data showed that the biomass proportion in stems increased with an increase in total biomass. Consequently, the biomass proportion in roots and leaves decreased with higher total biomass. Unlike the field data, however, allocation to the different plant parts did not change when the total biomass increased in NUCOM-tundra simulations.

S4.2.3 Fine root distribution

The cumulative root fractions over the soil layers were visually compared with simulated cumulative root fractions in NUCOM-tundra for early and late season. For graminoids, only field data from mixed and graminoid dominated plots, whereas for shrubs only field data from mixed and shrub dominated plots were used. In NUCOM-tundra, fine root distribution is determined by making use of a rooting depth coefficient β (Eq. S10 in Model Description; Gale and Grigal, 1987; Jackson et al., 1996). The fine root distribution in the model changes during the growing season along with changes in

active layer depths. Therefore, the NUCOM-tundra fine root distribution was determined for both graminoids and shrubs for three different active layer depths: 15cm, 30cm and 45cm.

The cumulative root biomass for both field data and model simulations is illustrated in Fig. S4.3 for shrubs and in Fig. S4.4 for graminoids. The root distribution for dwarf shrubs is very similar throughout the season both in shrub-dominated and mixed vegetation plots. Root distributions simulated in NUCOM-tundra for shrubs (using a rooting depth coefficient of β = 0.85) are well in the range of the observed cumulative root biomass in the field. A larger variation appears in the cumulative root distribution patterns for graminoids (Fig. S4.4). Both the active layer thickness and the total graminoid biomass have an effect on the root distribution, and thus cause the variation in root distribution in different seasons and vegetation types. The field data showed that graminoids root as deep as the active layer depth, which implies that late in the growing season a larger root biomass proportion is present in the deeper soil layers. Furthermore, a higher total graminoid biomass might result in a deeper rooting depth (Arora and Boer, 2003). Indeed, the roots sampled in graminoid dominated plots in late season showed deeper profiles compared to mixed vegetation plots (Fig. S4.4). The rooting depth coefficient for graminoids (β = 0.938) predicts the variation in fine root distribution for graminoids in mixed sites well, but the graminoid fine root biomass is estimated too high for the top soil layers in graminoid dominated plots. NUCOM-tundra includes only the effect of the active layer thickness on the fine root distribution and not the effect of biomass. Both observations and simulations show a clear difference in rooting pattern between dwarf shrubs and graminoids, with a shallow rooting pattern in dwarf shrubs and a relatively deep rooting pattern in graminoids which follows increases in active layer thickness.

References

Arora, V. K., and Boer, G. J.: A representation of variable root distribution in dynamic vegetation models, Earth Interactions, 7, 1-19, 2003.

Berendse, F.: Een simulatiemodel als hulpmiddel bij het beheer van vochtige heidevelden, CABO, Wageningen, NL, 1988.

5   Berendse, F.: Litter decomposition - a neglected component of plant fitness, Journal of Ecology, 82, 187-190, 1994a.

Berendse, F.: Competition between plant populations at low and high nutrient supplies, Oikos, 71, 253-260, 1994b.

Blok, D., Heijmans, M. M. P. D., Schaepman-Strub, G., Kononov, A. V., Maximov, T. C., and Berendse, F.: Shrub expansion may reduce summer permafrost thaw in Siberian tundra, Global Change Biology, 16, 1296-1305., 2010.

Essery, R., and Pomeroy, J.: Vegetation and topographic control of wind-blown snow distributions in distributed and
10 aggregated simulations for an Arctic tundra basin, Journal of Hydrometeorology, 5, 735-744, 2004.

Gale, M. R., and Grigal, D. F.: Vertical root distributions of northern tree species in relation to successional status, Canadian Journal of Forest Research, 17, 829-834, 1987.

Hargreaves, G. H., and Allen, R. G.: History and evaluation of Hargreaves evapotranspiration equation, Journal of Irrigation and Drainage Engineering, 129, 53-63, 2003.

15 Heinen, M.: Simplified denitrification models: overview and properties, Geoderma, 133, 444-463, 2006.

Heijmans, M. M. P. D., Mauquoy, D., van Geel, B., and Berendse, F.: Long-term effects of climate change on vegetation and carbon dynamics in peat bogs, Journal of Vegetation Science, 19, 307-320, 2008.

Jackson, R. B., Canadell, J., Ehleringer, J. R., Mooney, H. A., Sala, O. E., and Schulze, E. D.: A global analysis of root distributions for terrestrial biomes, Oecologia, 108, 389-411, 1996.

20 Kane, D. L., Hinzman, L. D., and Zarling, J. P.: Thermal response of the active layer to climatic warming in a permafrost environment, Cold Regions Science and Technology, 19, 111-122, 1991.

Kirschbaum, M. U.: The temperature dependence of soil organic matter decomposition, and the effect of global warming on soil organic C storage, Soil Biology and biochemistry, 27, 753-760, 1995.

Klein Tank, A. M. G., Wijngaard, J. B., Können, G. P., Böhm, R., Demarée, G., Gocheva, A., Mileta, M., Pashiardis, S., Hejkrlik, L., Kern-Hansen, C., Heino, R., Bessemoulin, P., Müller- Westermeier, G., Tzanakou, M., Szalai, S., Pálsdóttir, T., Fitzgerald, D., Rubin, S., Capaldo, M., Maugeri, M., Leitass, A., Bukantis, A., Aberfeld, R., Van Engelen, A. F. V., Forland, E., Mietus, M., Coelho, F., Mares, C., Razuvaev, V., Nieplova, E., Cegnar, T., Antonio López, J., Dahlström, B., Moberg, A., Kirchhofer, W., Ceylan, A., Pachaliuk, O., Alexander, L. V., and Petrovic, P.: Daily dataset of 20th-century surface air temperature and precipitation series for the European Climate Assessment, International journal of climatology, 22, 1441-1453, 2002.

Marion, G. M., and Miller, P. C. (1982). Nitrogen mineralization in a tussock tundra soil. *Arctic and alpine research*, 287-293.

Roebber, P. J., Bruening, S. L., Schultz, D. M., and Cortinas Jr, J. V.: Improving snowfall forecasting by diagnosing snow density, Weather and Forecasting, 18, 264-287, 2003.

Sistla, S. A., Moore, J. C., Simpson, R. T., Gough, L., Shaver, G. R., and Schimel, J. P. (2013). Long-term warming restructures Arctic tundra without changing net soil carbon storage. *Nature*, *497*(7451), 615-618.

van der Molen, M. K., van Huissteden, J., Parmentier, F. J. W., Petrescu, A. M. R., Dolman, A. J., Maximov, T. C., Kononov, A. V., Karsanaev, S. V., and Suzdalov, D. A.: The growing season greenhouse gas balance of a continental tundra site in the Indigirka lowlands, NE Siberia, Biogeosciences, 4, 985-1003, 2007.

van Oene, H., Berendse, F., and de Kovel, C. G. F.: Model analysis of the effects of historic CO2 levels and nitrogen inputs on vegetation succession, Ecological Applications 9, 920-935, 1999.

Walker, D. A., Raynolds, M. K., Daniels, F. J. A., Einarsson, E., Elvebakk, A., Gould, W. A., Katenin, A. E., Kholod, S. S., Markon, C. J., Melnikov, E. S., Moskalenko, N. G., Talbot, S. S., and Yurtsev, B. A.: The circumpolar Arctic vegetation map, Journal of Vegetation Science, 16, 267-282, 2005.

Zheng, D., Hunt Jr, E. R., and Running, S. W.: A daily soil temperature model based on air temperature and precipitation for continental applications, Climate Research, 2, 183-191, 1993.
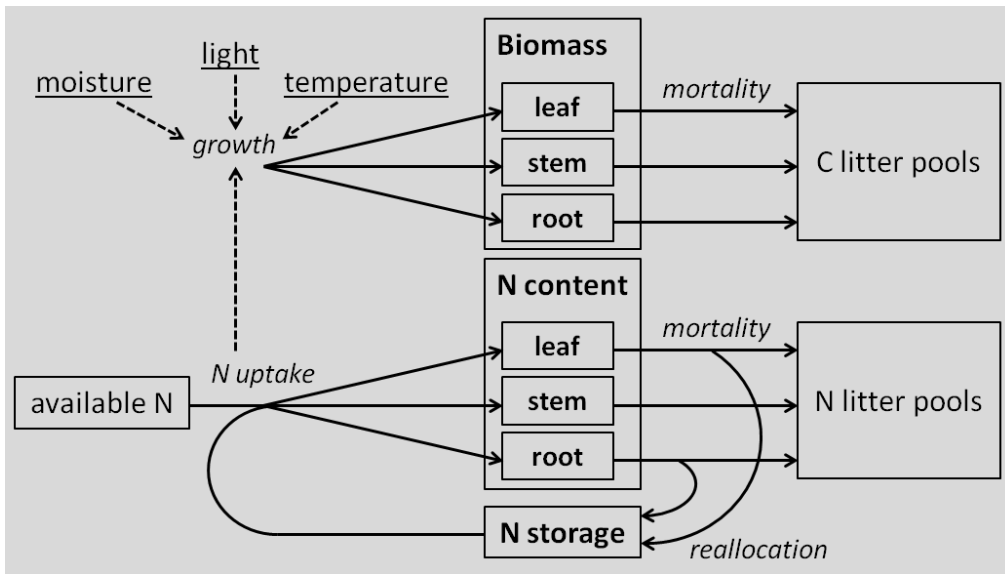
Figure S1.1. Overview of the main processes and growth factors for vascular plants in NUCOM-tundra. Biomass and nitrogen are separately simulated for all plant parts in graminoids and dwarf shrubs.
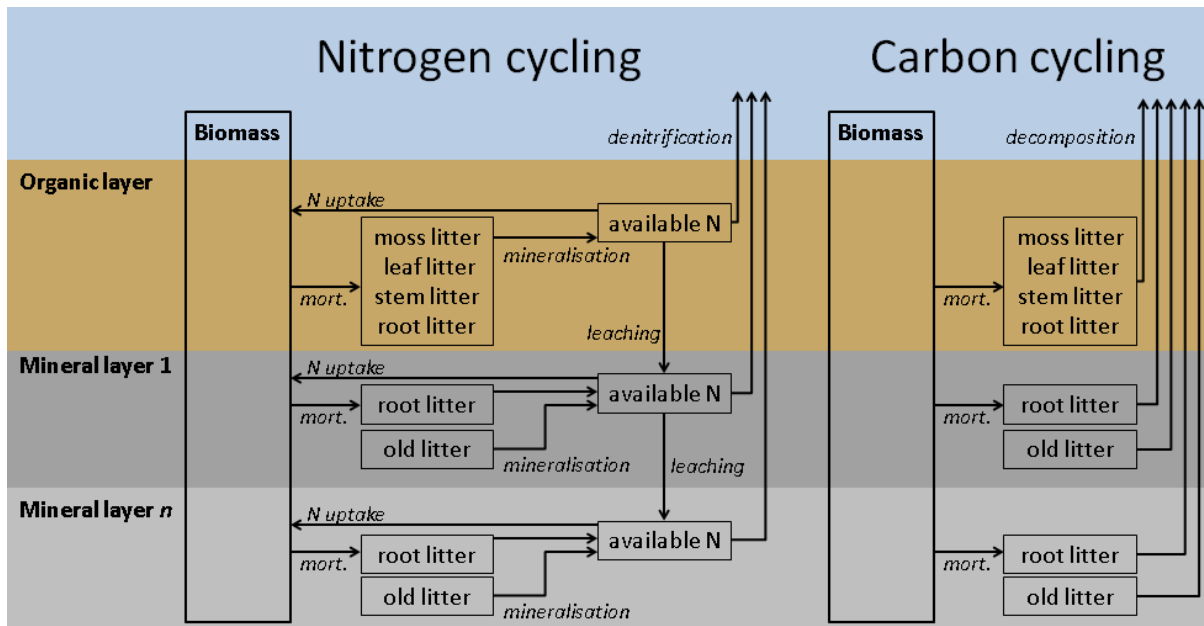
Figure S1.2. Overview of the soil nitrogen and carbon cycling variables and associated soil processes. Leaf, stem and root litter pools are separately simulated for graminoids and dwarf shrubs. Part of the nitrogen in dying vascular plant leaves and roots is allocated to the plant storage instead of transferred to the litter pools (not drawn here).
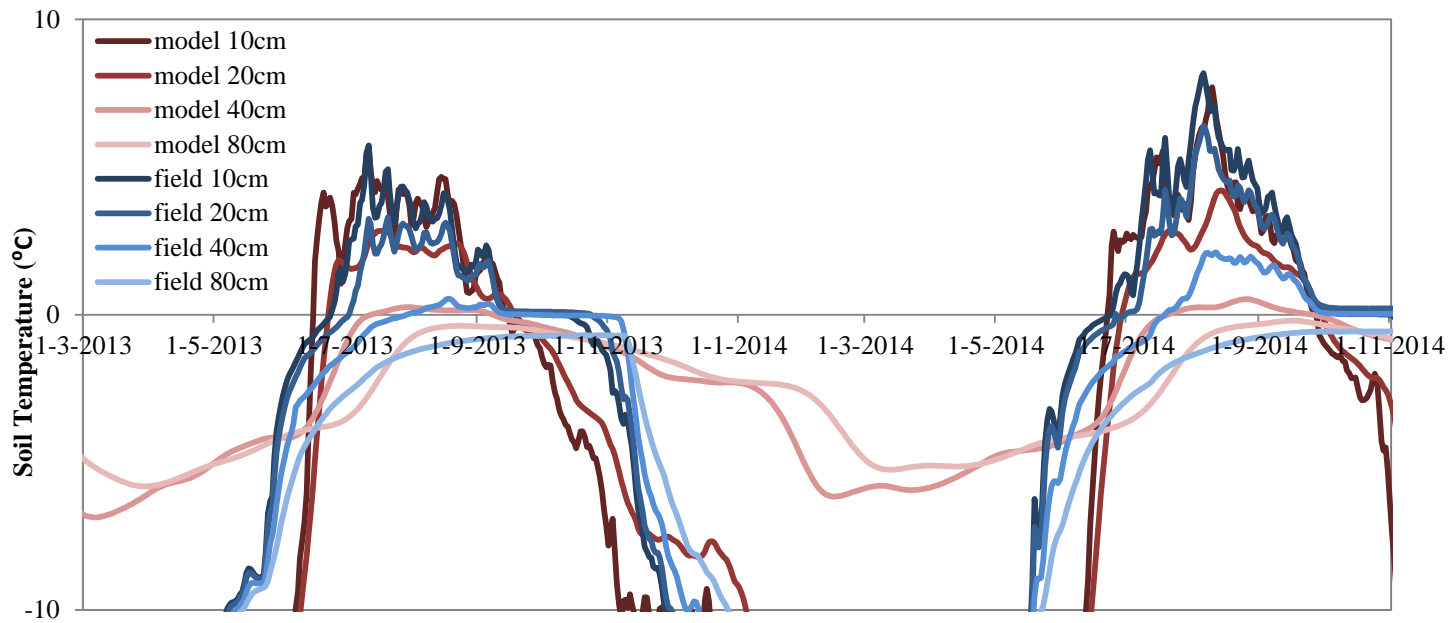
Figure S1.3. Simulated and observed soil temperatures for the growing seasons of 2013 and 2014. Field data were from Kytalyk field station in NE-Siberian tundra. Note that we focused on summer soil temperatures and only used summer field data to calibrate the regression functions.
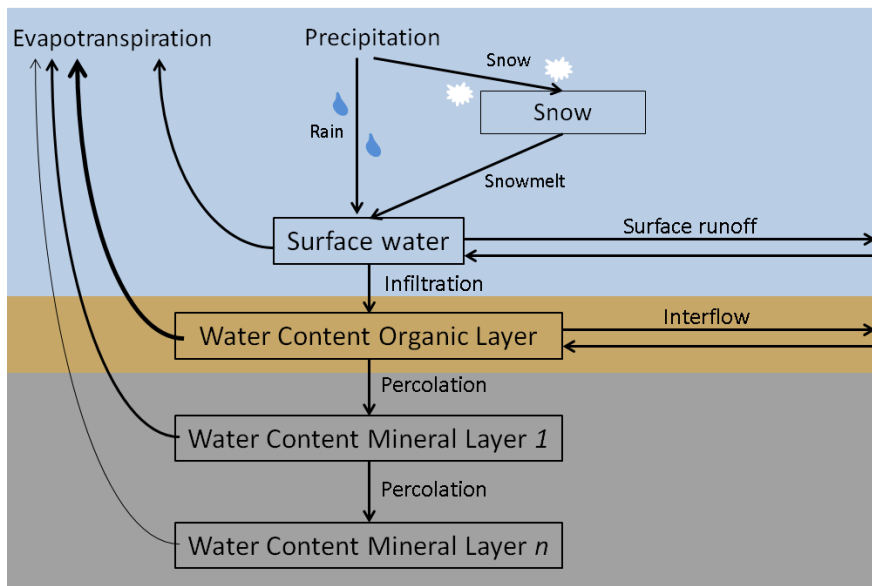
Figure S1.4. Overview of the hydrological variables and processes included in NUCOM-tundra.
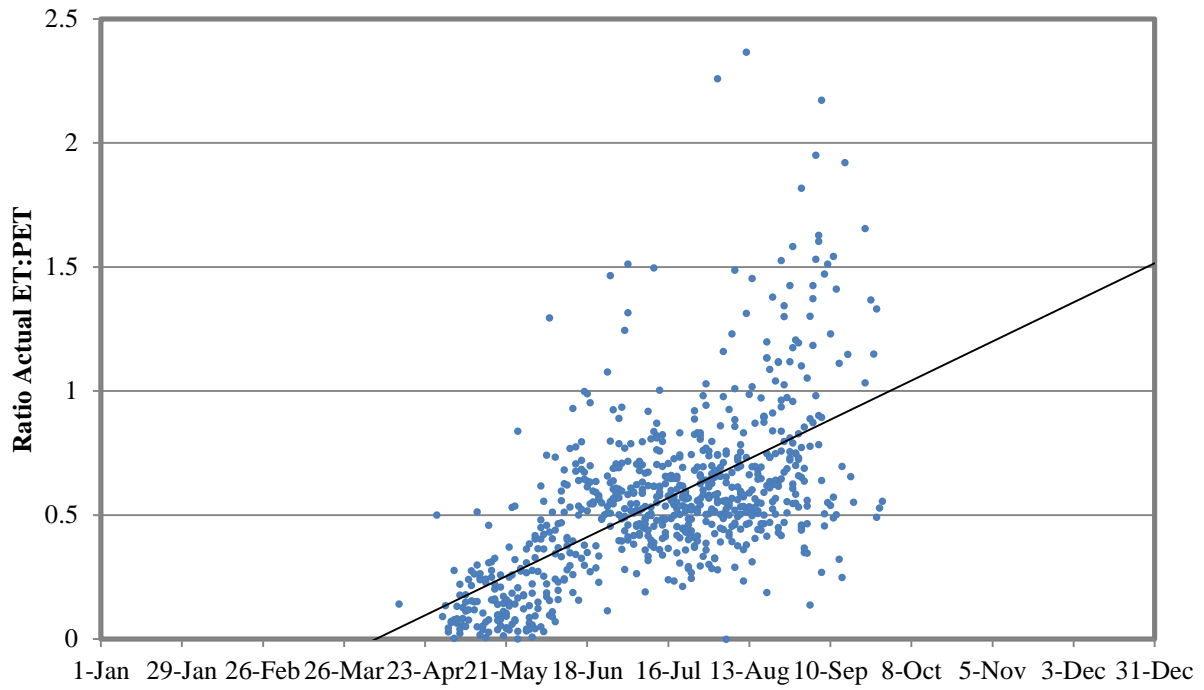
Figure S1.5. Actual evapotranspiration measured as latent heat flux at the Kytalyk field station divided by calculated Hargreaves potential evapotranspiration for 772 days in the time period 2003-2010.
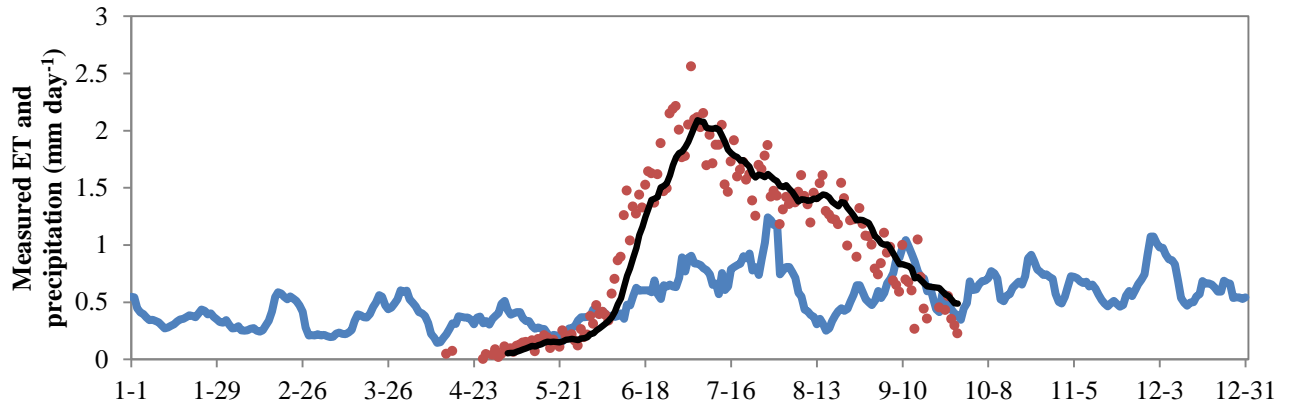
Figure S2.1. Measured daily evapotranspiration at Chokurdakh Tundra Station (red dots) for 772 days in 2003-2011 with 10-day averaged trend (black line) (data provided by VU research group) and the 10-day average precipitation (blue line) in
5   2003-2011 at the Chokurdakh Weather Station (Klein Tank et al., 2002). Both evapotranspiration and precipitation data are shown in mm day-1.
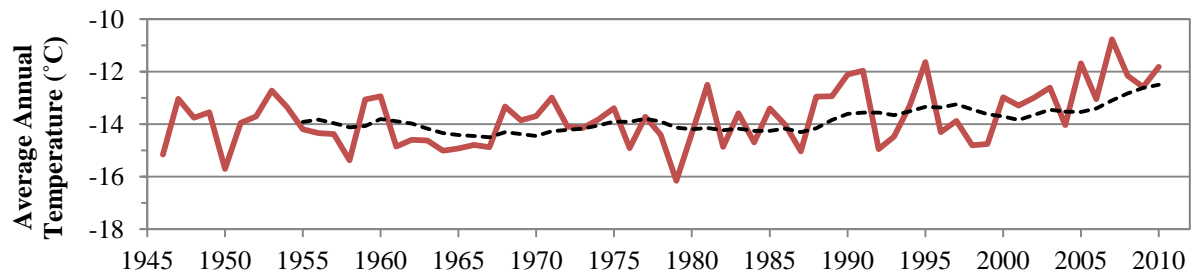
Figure S2.2. Average annual temperature (˚C) (solid line) with 10 year moving average (interrupted line) at the Chokurdakh Weather Station 1946-2010 (Klein Tank et al., 2002).
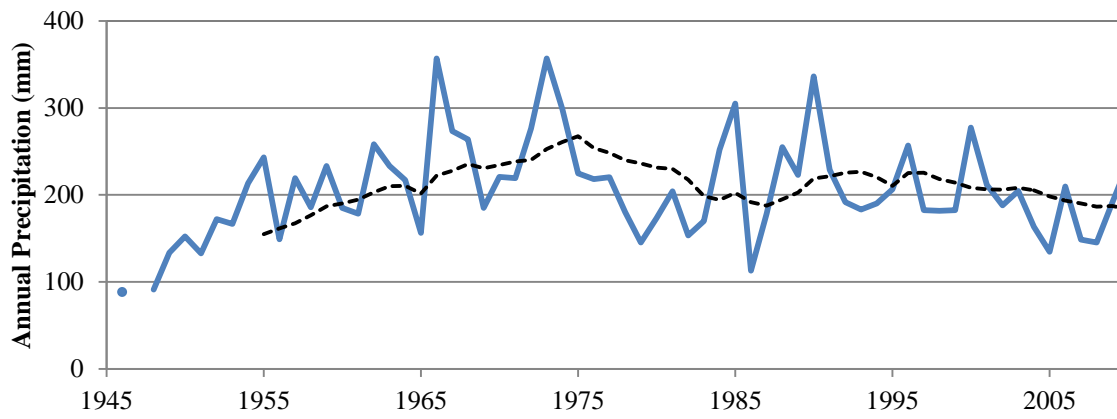
Figure S2.3. Annual precipitation (mm) (solid line) with 10 year moving average (interrupted line) at Chokurdakh Weather Station 1946-2010 (Klein Tank et al., 2002).
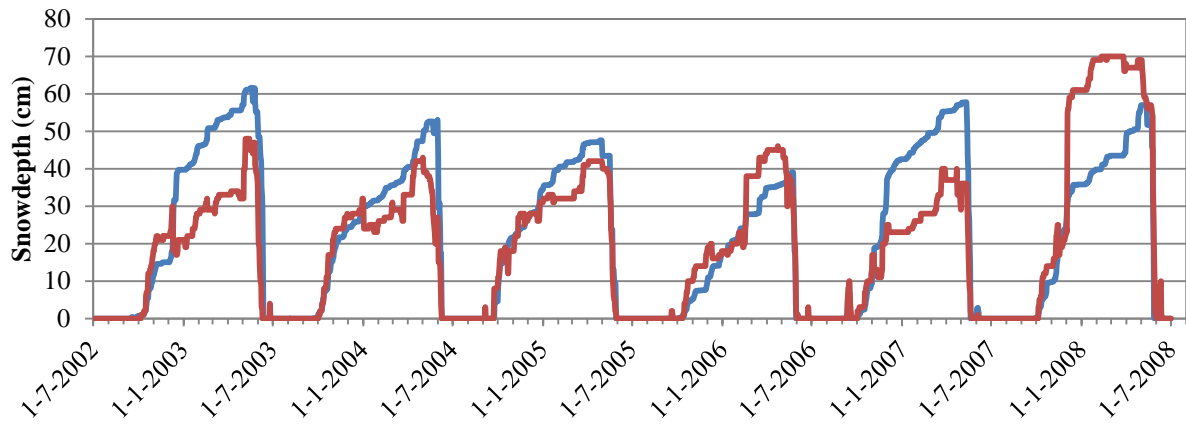
Figure S4.1. Snow depths in cm simulated with NUCOM-tundra (blue line) and measured at the Chokurdakh weather station (red line) from July 2002 till June 2008.
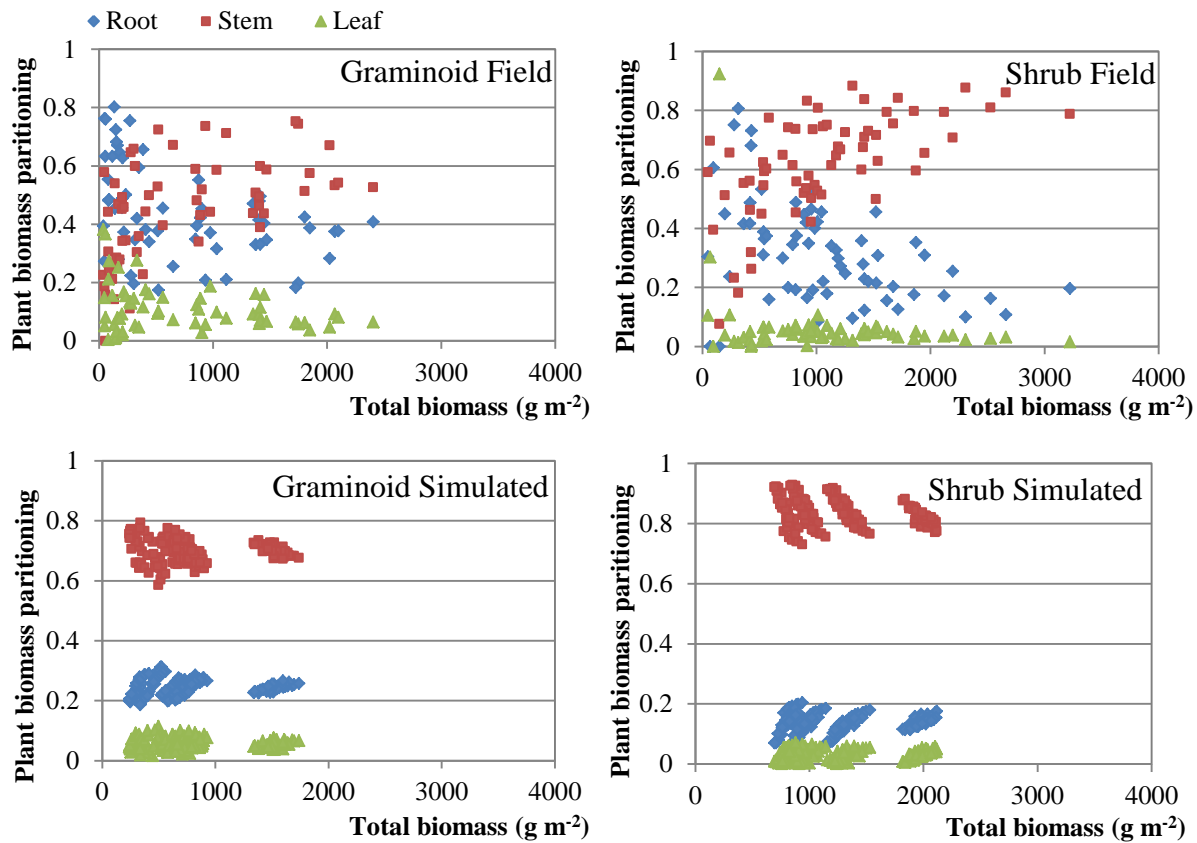
Figure S4.2. Comparison of field-based and simulated plant biomass proportions for graminoids and shrubs. For graminoids, only field samples and simulations in mixed and graminoid dominated plots were included, whereas for shrubs only samples and simulations in mixed and shrub dominated plots were included.
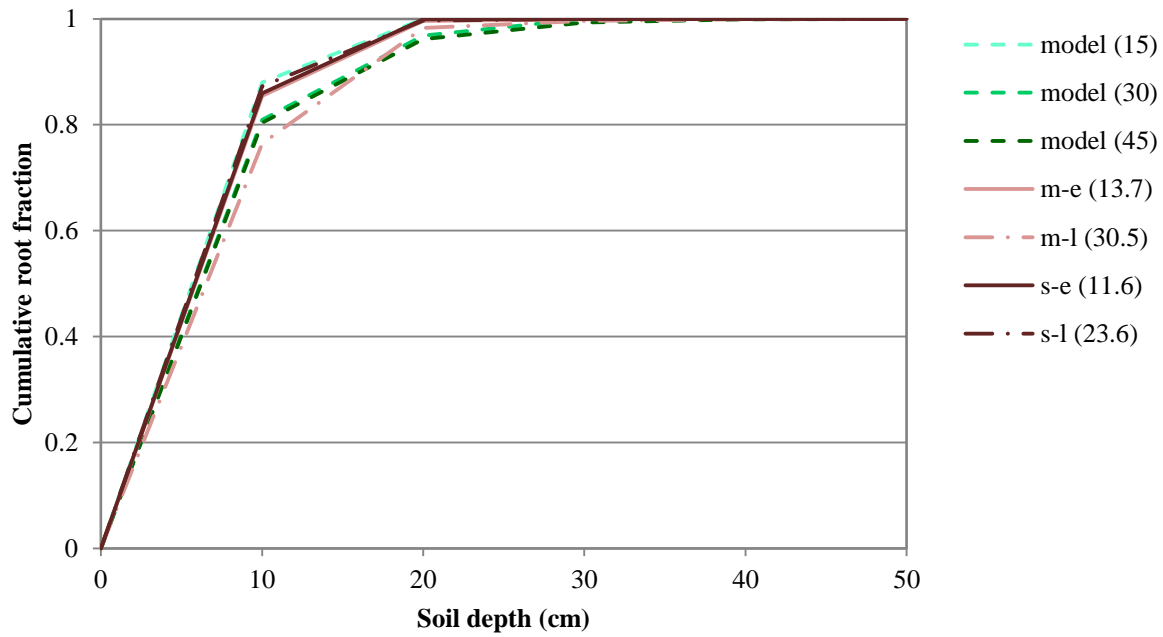
Figure S4.3. Cumulative distribution of shrub fine root biomass over soil depth simulated in NUCOM-tundra (green lines) and observed in field plots (red lines). Fine root distribution is simulated with β=0.85 and for different active layer depths. Field data is shown for shrub dominated (s) and mixed vegetation (m) plots, both in early (e) and late (l) season. The average measured ALT is displayed between brackets for all series.
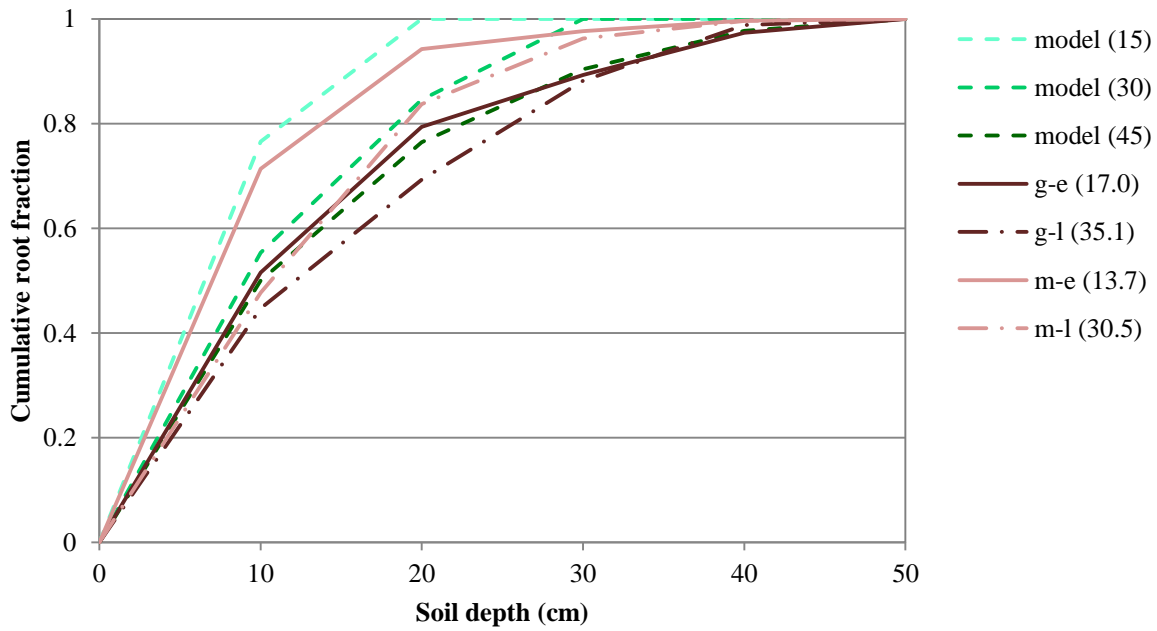
Figure S4.4. Cumulative distribution of graminoid fine root biomass over soil depth simulated in NUCOM-tundra (green lines) and observed in field plots (red lines). Fine root distribution is simulated with β=0.938 and for different active layer depths. Field data is shown for graminoid dominated (g) and mixed vegetation (m) plots, both in early (e) and late (l) season.

5   The average measured ALT is displayed between brackets for all series.

Table S1.1. Overview of ai and bi parameter values used to calculate soil temperatures at deeper depths (depth in cm).

depth	a_i	b_i
20	0.70	-0.40
30	0.60	-0.30
40	0.40	-0.25
50	0.94	-0.18
60	0.94	-0.16
70	0.94	-0.14
80	0.94	-0.12
90	0.94	-0.10
100	0.94	-0.09
110	0.94	-0.08
120	0.94	-0.07
130	0.94	-0.06
140	0.94	-0.05

Table S2.1. Annual and monthly averages of air temperature and precipitation at the Chokurdakh weather station during 1981-2010 (Klein Tank et al., 2002).

	Air T (°C)	Prec (mm)
Jan	-33.9	10.2
Feb	-32.7	10.1
Mar	-27.5	9.4
Apr	-18.4	7.1
May	-5.3	11.3
Jun	5.8	24.0
Jul	10.6	28.2
Aug	7.7	29.6
Sep	1.2	22.8
Oct	-11.5	20.1
Nov	-24.7	17.1
Dec	-31.6	13.6
Year	*-13.3*	*203.5*

Table S3.1. Moisture and litter start values in the mineral layers.

Mineral layer nr	watercontent (mm)	Na (g)	Nold (g)	N_litter_g_r_min (g)	N_litter_s_r_min (g)	Cold(g)	C_litter_g_r_min (g)	C_litter_s_r_min (g)
1	45	0.1	221	2	2	4652	2	2
2	45	0.1	188	2	2	4029	2	2
3	45	0.1	190.5	2	2	3969	2	2
4	45	0.1	224	2	2	4144	2	2
5	45	0.1	284	2	2	4799	2	2
6	45	0.1	366	2	2	5835	2	2
7	45	0.1	465.5	2	2	7270	2	2
8	45	0.1	578	2	2	9130	2	2
9	45	0.1	699	2	2	11335	2	2
10	45	0.1	824	2	2	13965	2	2

Table S3.2. Water flows and initial biomass of PFTs in the five vegetation types simulated in NUCOM-tundra.

	1: Shrub dry	2: Shrub moist	3: Mixed moist	4: Graminoid moist	5: Graminoid wet
Hydrology					
Surface Runoff out	yes	yes	yes	Yes	no
Surface Runoff in	no	yes	yes	Yes	yes
Interflow out	yes	yes	yes	Yes	no
Interflow in	no	yes	yes	Yes	yes
Vegetation					
Shrub	1500g	1125g	750g	375g	-
Graminoid	-	250g	500g	750g	1000g
Moss	250g	250g	250g	250g	250g